

PERFORMANCE ANALYSIS OF MULTI-RELAY FREE SPACE OPTICAL COMMUNICATION SYSTEMS

A Thesis

by

Zohreh Mostaani

Submitted to the
Graduate School of Sciences and Engineering
In Partial Fulfillment of the Requirements for
the Degree of

Master of Science

in the
Department of Electrical and Electronics Engineering

Özyeğin University
January 2015

Copyright © 2015 by Zohreh Mostaani

PERFORMANCE ANALYSIS OF MULTI-RELAY FREE SPACE OPTICAL COMMUNICATION SYSTEMS

Approved by:

Professor Murat Uysal, Advisor
Department of Electrical and Electronics
Engineering
Özyeğin University

Professor Cenk Demirođlu
Department of Electrical and Electronics
Engineering
Özyeğin University

Professor Niyazi Odabaşođlu
Department of Electrical and Electronics
Engineering
Istanbul University

Date Approved: 8 January 2015

To my parents

ABSTRACT

Free space optical (FSO) communication has attracted a great attention in recent years because of their high bandwidth capacity in unregulated spectrum which makes them a cost-effective and easy-to-install alternative to fiber optics. Moreover they provide high immunity to interference and jamming due to directional and narrow beams. FSO systems are appealing for number of applications including last-mile access, fiber back-up, back-haul for wireless cellular networks, and disaster recovery among others. The major degrading factor in these systems is atmospheric turbulence induced fading particularly for long range links. Relay-assisted FSO systems provide significant performance gains by using the advantage of shorter hops and the fact that fading variance is distance dependent in FSO channels. In this thesis, we investigate the performance of multi-relay FSO systems in various settings. In the first part of thesis, we consider an all-optical relaying system to remove the need for optical -electrical- optical conversions. We explore the benefits of relay selection and investigate its outage performance over Gamma-Gamma distributed turbulence channels. In the second part of thesis, we assume that source is equipped with multiple transmit apertures employing the so-called spatial pulse position amplitude modulation (SPPAM). We investigate an upper bound for bit error rate of this system with multiple parallel relays over log-normal distributed channels.

ÖZETÇE

Serbest Uzay Optik (SUO) İletişimi, son yıllarda, düzenlenmemiş spektrumda yüksek bant genişliği kapasitesi sağlaması onu, fiber optik iletişimin, uygun maliyetli ve kolay kurulabilir bir alternatifi yaptığından, büyük bir ilgi görmüştür. Üstelik, yönlendirilmiş ve dar hüzmeler sayesinde girişim ve parazitlenmeye karşı yüksek bağıklık sağlarlar. SUO sistemleri, son mil erişimi, fiber yedekleme ve kablosuz hücresel ağları için back-haul olmayı içeren bir çok uygulamaya olanak sağlaması ve felaket telafisi özelliklerinden dolayı, diğer sistemler arasında caziptir. Bu sistemlerde en önemli bozucu etmen, özellikle uzun mesafe hatları için, atmosferik türbülans tarafından uyarılmış sönümlenmedir. Röle destekli SUO sistemleri kısa atlamaların avantajını kullanarak ve SUO kanallarında sönümlenme varyansının mesafeye bağlı olmasından dolayı, yüksek başarımlı kazancı sağlar. Bu tezde, çok röleli SUO sistemlerinin başarımlarını, farklı ayarlamalarda inceledik. Tezin birinci kısmında, optik-elektrik-optik dönüşüm ihtiyacını ortadan kaldırmak için, tüm-optik röle sistemini göz önünde bulundurduk. Röle seçiminin etkisini araştırdık ve bunun Gamma-Gamma dağılıma sahip türbülans kanalları üzerindeki hizmet kesilme başarımlarını inceledik. Tezin ikinci kısmında, kaynağın, uzamsal darbe konum genlik kiplemesini (UDKGGK) kullanan çoklu verici açıklıkları ile donatılmış olduğunu varsaydık. Bu sistemin bit hata oranı için, log-normal dağılımlı kanallar üzerinde çoklu paralel rölelerle, bir üst sınırı araştırdık.

ACKNOWLEDGEMENTS

I would like to foremost thank my supervisor Professor Murat Uysal whose support, guidance, encouragement, and immense knowledge have been key factors to accomplish this work. It is an honor for me to study and research under his supervision.

I would like to sincerely acknowledge my thesis defense committee members, Professor Cenk Demirođlu and Professor Niyazi Odabaşıođlu for spending their precious time.

My warmest gratitude goes to my parents and brothers whose their support and love has given me the opportunity to follow my dreams. I also would like to thank my partner in life, Amir Mohammadi for his unconditional love and support during this work.

Finally, I would like to extend my thanks to my wonderful friends and lab mates with whom I shared many happy moments of my life.

TABLE OF CONTENTS

DEDICATION	iii
ABSTRACT	iv
ÖZETÇE	v
ACKNOWLEDGEMENTS	vi
LIST OF TABLES	ix
LIST OF FIGURES	x
I INTRODUCTION	1
1.1 Overview of FSO Communications	1
1.2 Atmospheric Turbulence	2
1.3 Fading Mitigation Tools	4
1.3.1 Error Correcting Codes	5
1.3.2 Maximum Likelihood Sequence Detection	5
1.3.3 Spatial Diversity	5
1.3.4 Multiuser Diversity	6
1.3.5 Relay-assisted Communication	6
1.4 Thesis Motivation	8
1.4.1 All Optical Relaying	8
1.4.2 Spatial Modulation	9
1.5 Thesis Structure and Contributions	10
II RELAY SELECTION IN FSO SYSTEMS WITH ALL-OPTICAL RELAYING OVER GAMMA-GAMMA TURBULENCE CHANNELS	12
2.1 Channel and System Models	12
2.2 Outage Performance Analysis	15
2.3 Numerical Results and Discussions	17

III RELAY-ASSISTED SPATIAL PULSE POSITION AMPLITUDE MODULATION IN FSO	21
3.1 Performance Analysis	24
3.1.1 Calculating Average Pairwise Error Probability(\overline{PEP})	25
3.1.2 Defining Error Types	27
3.2 Numerical Results and Discussions	31
IV CONCLUSIONS AND FUTURE DIRECTIONS	35
REFERENCES	37
VITA	43

LIST OF TABLES

LIST OF FIGURES

1	The block diagram of an optical communication system.	1
2	System model of a cooperative relaying system with N relays.	13
3	Mathematical model for transmission through one relay.	15
4	Outage probability of all-active and max-min protocol for full-CSI cooperative relaying system with different number of relays over Gamma-Gamma channels.	18
5	Outage probability of all-active and max-min protocol for semi-blind cooperative relaying system with different number of relays over Gamma-Gamma channels.	19
6	Outage probability of all-active and max-min protocol for full-CSI cooperative relaying system with different values of DoF over Gamma-Gamma channels.	19
7	Outage probability of all-active and max-min protocol for semi-blind cooperative relaying system with different values of DoF over Gamma-Gamma channels.	20
8	System with SPPAM in source and relays between source and destination.	22
9	SPPAM mapping rule for system with $N_t = 8$, $M = 4$ and $Q = 2$. . .	23
10	Average BER of a system with SPPAM in source and different number of relays over log-normal channels.	32
11	Average BER of systems with $N = 4$ relays and spectral efficiency of 3 bits/s/Hz with different number of transmit antennas in source over log-normal channels.	33
12	Average BER of systems with $N = 4$ relays and spectral efficiency of 3 bits/s/Hz with different number of transmit antennas in source over log-normal channels.	34

CHAPTER I

INTRODUCTION

Free space optical (FSO) communication involves the use of optical carriers for wireless connectivity between two fixed points [1]. In this chapter, we first provide an overview of FSO communication and discuss about the atmospheric turbulence induced fading which is a major performance limiting factor. Then, we discuss on how to improve FSO system performance in the presence of atmospheric turbulence. We further elaborate on relay-assisted FSO communication which has been recently proposed as powerful fading mitigation tool and forms the basis of this thesis.

1.1 Overview of FSO Communications

In FSO communication systems a source produces information waveforms which will be modulated onto an optical carrier. The generated optical field will be radiated through an optical channel (atmospheric turbulence) towards a destination. At the receiver, the field is optically collected and a photo-detector transforms the optical field to an electrical current. The receiver processes the detected electrical current to recover the original transmitted information [2].

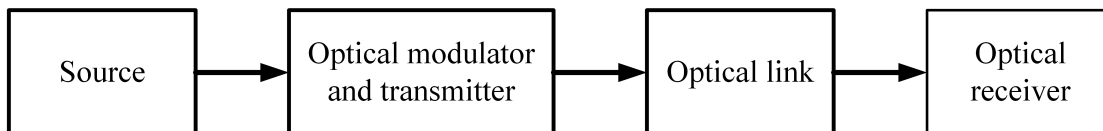


Figure 1: The block diagram of an optical communication system.

Direct detection (non-coherent) receivers are so practical in FSO systems because of their simple and cost-effective implementation. In these receivers, the photodetector directly detects the instantaneous power (intensity) of the collected field at the

receiver aperture so they can only be employed in intensity modulation direct detection (IM/DD) systems where the information is contained in the intensity variation of optical field.

FSO systems offer very high data speeds comparable to fiber optics [3]. Since they operate in unregulated spectrum, there is no need to pay license fee. Very narrow beams used in lasers offer significant advantages over RF counterparts such as enhanced security, decreased power consumption and lower electromagnetic interference [3–6].

Transferring high data rate from optical fiber backbone to the clients is usually problematic because it is expensive and time consuming and sometimes not possible to lay down fiber optics in an urban area. FSO communication is an efficient solution for this last mile problem because of their high data rate, easy installation and quick deployment [7]; they are also easily redeployable which makes them a good candidate for systems that are subject to frequent changes in their configuration or architecture.

The performance of terrestrial FSO systems is degraded by some atmospheric effects including absorption and scattering of the laser beam in adverse weather condition such as rain or fog [8]. Building sways because of wind load, thermal expansion and small earthquakes may also cause to cut off the communication [9]. Another major impairment is from the atmospheric turbulence particularly for link ranges longer than 1 kilometer [6, 10, 11].

1.2 Atmospheric Turbulence

Atmospheric turbulence occurs as a result of inhomogeneities in the temperature and pressure of the atmosphere which cause variations of the refractive index along the transmission path. This consequently leads to random fluctuations in phase and intensity (irradiance) of the received signal. These fluctuations can severely deteriorate the performance of FSO communication systems [12, 13]. The coherence

time of atmospheric turbulence fading depends on wind velocity, and can be on the order of milliseconds which is greater than the symbol duration in each transmission, therefore optical channels are slow-fading channels [14–16]. Scintillation index is typically used to measure turbulence strength and given by

$$\sigma_I^2 = \frac{E[I^2]}{E[I]^2} - 1 \quad (1)$$

where $E[.]$ is the irradiance (intensity) of the optical wave and is the ensemble average [17].

Plane wave and spherical wave (point source) are two asymptotic regimes for optical waves that can be characterized by Rytov variance

$$\sigma_R^2 = 1.23C_n^2 k^{7/6} L^{11/6} \quad (2)$$

where C_n^2 ($\text{m}^{-2/3}$) stands for the refractive index parameter, $k = 2\pi/\lambda$ and λ (m) is the wavelength. L (m) is the distance between transmitter and receiver. Rytov variance is a measure of turbulence optical strength and is being used to characterize irradiance fluctuation from weak for Rytov variance less than unity ($\sigma_R^2 < 1$) to moderate to strong for Rytov variance greater than unity ($\sigma_R^2 \geq 1$) [5]. Let $\sigma_{I_{pl}}^2$ and $\sigma_{I_{sp}}^2$ denote the scintillation index of respectively plane and spherical waves. In terms of Rytov variance, they are expressed as

$$\sigma_{I_{pl}}^2 = \sigma_R^2 = 1.23C_n^2 k^{7/6} L^{11/6} \quad (3)$$

$$\sigma_{I_{sp}}^2 = 0.4\sigma_R^2 = 0.5C_n^2 k^{7/6} L^{11/6} \quad (4)$$

The typical value for refractive index varies from approximately $10^{-17} \text{ m}^{-2/3}$ for weak turbulence conditions to $10^{-13} \text{ m}^{-2/3}$ for strong turbulence conditions.

There are several statistical models to describe the behavior of random irradiance. Some of the known distribution models are Rice-Nakagami distribution, log-normal distribution, K-distribution and Gamma-Gamma distribution [8]. Among these, the

most popular distribution for weak turbulence channels is log-normal and for moderate to strong turbulence channels is Gamma-Gamma distribution.

The probability density function (PDF) for a log-normal channel is given as

$$f(I) = \frac{1}{I\sqrt{2\pi\sigma_I^2}} \exp\left(-\frac{(\ln(I) - \mu_I)^2}{2\sigma_I^2}\right), I > 0 \quad (5)$$

where μ_I and σ_I^2 are mean and variance of intensity respectively. On the other hand, the PDF of Gamma-Gamma distribution [18] is given by

$$f(I) = \frac{2(\alpha\beta)^{(\alpha+\beta)/2}}{\Gamma(\alpha)\Gamma(\beta)\bar{I}} \left(\frac{I}{\bar{I}}\right)^{\frac{(\alpha+\beta)}{2}-1} K_{\alpha-\beta} \left[2\sqrt{\alpha\beta \left(\frac{I}{\bar{I}}\right)}\right] \quad (6)$$

where \bar{I} denotes the average irradiance, $K_\nu(\cdot)$ is the modified Bessel function of the second kind and order ν , $\Gamma(\cdot)$ is the Gamma function. α and β represent the effect of large-scale and small-scale cells of a spherical wave and are given by

$$\alpha = \left[\exp\left(\frac{0.49\beta_0^2}{\left(1 + 0.18d^2 + 0.56\beta_0^{12/5}\right)^{7/6}}\right) - 1 \right]^{-1} \quad (7)$$

$$\beta = \left[\exp\left(\frac{0.51\beta_0^2 \left(1 + 0.69\beta_0^{12/5}\right)^{-5/6}}{1 + 0.90d^2 + 0.62d^2\beta_0^{12/5}}\right) - 1 \right]^{-1} \quad (8)$$

where $\beta_0^2 = \sigma_{I,\text{sp}}^2(d) = 0.5C_n^2\kappa^{7/6}L^{11/6}$ is the Rytov parameter. In (7) and (8), $d = (kD^2/4L)^{1/2}$ characterizes the aperture averaging effect where D denotes the diameter of the receiver aperture.

1.3 Fading Mitigation Tools

Several mitigation tools has been introduced in literature to overcome the degrading effects of turbulence induced fading such as error correcting codes [19, 20], Maximum Likelihood Sequence Detection (MLSD) [21], spatial diversity [10, 22], multiuser schemes [23, 24], and relay-assisted communications [25, 26].

1.3.1 Error Correcting Codes

Error correcting codes add redundancy to the transmitted data and use these redundancies to detect error and immediately correct it on the receiver side. They need to deal with highly correlated channel states and therefore require large-size interleavers to achieve the desired performance. Block codes, convolutional codes and turbo codes are three schemes for linear error correcting codes

1.3.2 Maximum Likelihood Sequence Detection

MLSD with knowledge of joint temporal fading distribution needs multidimensional integrations which causes high computational complexity [10]. Some sub-optimal temporal-domain mitigation techniques has been proposed in [12, 27] which gives a solution when receiver only has knowledge of the marginal fading distribution, but knows neither the temporal fading correlation nor the instantaneous fading state.

1.3.3 Spatial Diversity

Spatial diversity involves using several apertures in transmitter and/or receiver side that can provide an attractive alternative approach for fading compensation with its inherent redundancy. This technique provides significant performance gains by introducing additional degrees of freedom in the spatial dimension and has been extensively studied in FSO communications [11, 23, 28, 29].

Using several apertures in transmitter, known as MISO (Multiple Input Single Output), gives transmit diversity advantage by duplicating signals over several optical beams [30, 31]. On the other hand, deployment of several apertures at receiver side is called SIMO (Single Input Multiple Output) and provides receive diversity advantages. Equal Gain Combining (EGC) or optimal Maximal-ratio Combining (MRC) [10, 23] can be employed to process the received signals. In an FSO system, receiver diversity can also be offered by one large lens to average over received fluctuations. This method called aperture averaging and can be efficiently employed if

the receiver lens aperture is larger than the fading correlation length [32].

Deployment of multiple transmit and receive apertures antennas is called MIMO (Multiple Input Multiple Output) which offers diversity gains as well as multiplexing gain [33]. Performance of MIMO FSO systems has been investigated over different turbulence channel models [10, 12, 23, 28, 34].

1.3.4 Multiuser Diversity

Multiuser diversity involves the selection of the user with the best channel quality and allocates the system resources to that user for a certain time slot. This method improves the system throughput and link reliability by taking advantage of the channel fluctuations particularly in systems where implementing MIMO techniques are challenging [35]. It has been shown that multiuser diversity can better improve the system performance with larger number of independent channels and hence number of users [36]. Systems employing multiuser techniques need a simpler receiver structure but they have some draw backs such as unfairness among users especially for the ones which are closer to the base station and requiring channel state information (CSI) in transmitter side for selection purposes [37].

1.3.5 Relay-assisted Communication

Relay-assisted FSO communication has been first introduced in [38] as an alternative approach to achieve spatial diversity. Unlike RF channels, the severity of small-scale fading in optical channels is distance dependent. Therefore using relays in FSO systems not only reduces the path-loss but also mitigates the fading effect of the turbulence channel. Moreover, since FSO communication is not a broadcasting technology, using relays is beneficial where there is no clear line of sight between source and destination.

Two processing techniques have been used for relaying in FSO systems, namely amplify-and-forward (AF) and decode-and-forward (DF) relaying. In AF relaying, the

relay multiplies the received signal with a proper energy scaling term and forwards it to the next relay or destination. On the other hand, in DF relaying, the relay decodes the received signal and then retransmits it to the next relay or destination.

There are two different configurations of relays in FSO communications whether they are employed in serial (multi-hop transmission) or parallel (cooperative diversity). In the first configuration, data transmits from source to relay node. Based on the AF or DF relaying method, each relay scale the received signal and forward it or decode and retransmit the signal to the next relay. This continues until sources data receives the destination. In the second configuration, source is equipped with multiple transmitters each of which pointing out in direction of corresponding relay node. The source transmits the same signal to all relays and relays send it to the destination. The main idea in cooperative diversity is that, by employing multiple relay nodes with line-of-sight (LOS) to both the source and the destination, a virtual multiple-aperture system is created. Advantage of this virtual multiple-aperture system, as opposed to MIMO FSO systems, is that multiple paths are spatially separated from each other, thus ensuring independence of the corresponding fading channels [39].

Performance of multi-hop transmission and cooperative diversity has been reported in literature. Bit error rate performance of serial relaying with DF relays has been investigated in [40] while the outage performance of such system under the assumption strong turbulence channels with AF relaying has been reported in [41]. On the other hand, the performance of a parallel relaying with single relay and a direct link assuming AF and DF relaying has been investigated in [6, 26] and [42]. Finally in [25] the outage performance of both relaying configurations (multi-hop transmission and cooperative diversity) with AF and DF relaying methods under the assumption of log-normal channel has been presented.

It should be emphasized that in most of mentioned works on parallel relaying, it is assumed that all relays are simultaneously active. Such systems where all the

relays participate in the relaying phase need strict synchronization among them. One way to overcome this problem is relay selection in which only one selected relay is active during the relaying phase. Performance of relay selection in FSO has been investigated in [39, 43] and [44]. In [43], an upper bound for average error probability has been derived over Rayleigh and lognormal fading channels. In [44], the average error performance of the DF system with relay selection over the Gamma-Gamma fading channels is derived. In [39], three different protocols namely select-max, all-active and distributed switch-and-stay have been proposed to select from relays over Gamma-Gamma channels. One of the most common-used protocols for selecting relays is max-min protocol which refers to the selection of the relay with the highest instantaneous signal-to-noise ratio (SNR).

1.4 Thesis Motivation

In this thesis we investigate the performance of cooperative FSO communications. First, we employ relay selection in system with all-optical relays between source and destination to increase the speed of communication. Then we use spatial modulation (SM) in transmitter with conventional relays to increase the spectral efficiency.

1.4.1 All Optical Relaying

In the initial studies on relay-assisted FSO systems [6, 25, 45], it is assumed that there are electrical-optical (EO) and optical-electrical (OE) at relay nodes. This requires high speed electronics and electro optics devices for implementation. All-optical relaying has been proposed in recent papers [46–49] where the signals are processed in optical domain eliminating the need for EO and OE conversions.

In [46] bit error rate performance of a dual-hop FSO system with optical AF relay has been investigated based on a photon counting approach and the effects of amplified spontaneous emission (ASE) noise, shot noise caused by background radiation and thermal noise in receiver has been considered while in [47], Bayaki et.

al investigated the outage performance of a multi-hop FSO system with optical and electrical amplification based on a general approach proposed in [50]. They took into account the effect of thermal noise, background radiation, ASE, various beat noises, and signal dependent noise. In [48] bit error rate performance of a multi-hop FSO system with optical AF and regenerative and forward relays has been investigated via Monte Carlo simulation and instead of optical intensity channels the complex field distributions at each relay were modeled in the presence of background noise. Finally in [49], they investigate the outage performance of a dual-hop AF relaying based on a photon counting methodology proposed in [51] and they considered the effect of ASE and Degree of Freedom (DoF).

In this thesis, we investigate the outage performance of a relays-assisted FSO communication system with multiple AF parallel relays. We consider the effect of ASE and DoF in relays and destination and employ relay selection in order to choose the relay with best channel quality to forward the signal to the destination.

1.4.2 Spatial Modulation

As discussed in [52–54], SM is a MIMO technique that only one antenna is active during each time slot, and the receiver is simpler. This modulation increases the data rate and spectral efficiency of a system without requiring any bandwidth expansion. The key point in SM is mapping information into two carrying information units. First one is the conventional signal constellation and second one is the spatial constellation which is the transmitter antenna arrays [55].

Space Shift Keying (SSK) [56] is a special form of SM where only the indices of transmit antenna is carrying the information. Even though SSK is spectrally efficient and has the minimum implementation cost, every single bit increment in the spectral efficiency requires doubling the number of transmitters. Using other signal modulation like Pulse Position Modulation (PPM) or Pulse Amplitude Modulation

(PAM) or both of them along with SSK has been investigated in [57–59] as a solution to this problem.

Application of SM has been widely investigated in RF and indoor optical wireless communications [60–62]. In [60] an upper bound for the average bit error rate of a MISO system over general fading channels has been described while in [61] the upper bound for a MIMO system over correlated Rayleigh and Rician channel has been investigated. In [62] performance of a MIMO indoor optical communication system has been described. Unlike RF and optical indoor communication, SM only recently has been considered in FSO systems over turbulence fading channels in [59]. In [59] an upper bound for bit error probability of a MIMO FSO system with spatial pulse position amplitude modulation (SPPAM) under weak to strong turbulence has been investigated.

A major drawback of SM is that the diversity gain is limited to the number of receiver antennas. One method to overcome this limitation is using cooperative diversity by employing relays between source and destination. The concept of using SM along with cooperative communication has been discussed in several RF literatures [63, 64]. In [63], the performance of a SSK system with one AF relay has been presented while in [64] the performance of SM with multiple DF relays has been presented.

In this thesis, we investigate an upper bound for bit error rate of a cooperative relay-assisted FSO system with multiple DF relays between source and destination where source is employing SPPAM to send the data over optical channel.

1.5 Thesis Structure and Contributions

In this thesis, we investigated the outage performance and bit error rate of various settings with relay assisted communication over different atmospheric turbulence conditions.

In chapter 2, we introduce a cooperative FSO system with number of parallel relays between source and destination. Relays optically amplify and forward the received signal to the destination. We investigate the outage probability of two protocols for relaying phase under the assumption of Gamma-Gamma turbulence channels. One protocol is when all relays are active and transmit the signal simultaneously and the other one is when only one relay with the maximum SNR (or best channel quality) has been selected to forward the signal to the destination.

In chapter 3, we consider a cooperative FSO system which employs number of parallel relaying path each of which with one DF relay between source and destination (cooperative communication). This system exploits SPPAM in the source. The active antenna transmits the signal to all the relays and those which decode the received signal correctly retransmit it to the destination. Under the assumption of log-normal turbulence channel we derived a closed form expression of an upper bound for average bit error rate of the described system, using average pairwise error probability (PEP) and union bound technique. The derived analysis is validated through Monte Carlo simulation results. Finally we conclude in chapter 4.

CHAPTER II

RELAY SELECTION IN FSO SYSTEMS WITH ALL-OPTICAL RELAYING OVER GAMMA-GAMMA TURBULENCE CHANNELS

In this Chapter, we consider an all-optical multi-relay FSO system and investigate its outage performance over Gamma-Gamma atmospheric turbulence channels. To avoid strict synchronization requirements among relay nodes, we employ relay selection and use only the selected relay in the relaying phase.

2.1 Channel and System Models

The system model under consideration is depicted in Fig.2. We consider a dual-hop FSO system with N parallel paths. The source node modulates and transmits the intensity-modulated signal. At the relay node, the received signals are optically filtered and amplified. Both pre- and post-filtering are utilized to minimize the effects of background and ASE noise of optical amplifiers. We consider the so-called max-min cooperation protocol [65] in which the best relay is chosen based on the following metric

$$R_b = \arg \max_{i \in \{1, 2, \dots, N\}} \{\min(\gamma_{0,i}, \gamma_{i,N+1})\} \quad (9)$$

where $\gamma_{0,i}$ is the instantaneous SNR between the source and the i^{th} relay and $\gamma_{i,N+1}$ is the instantaneous SNR between the i^{th} relay and the destination.

To implement this cooperation protocol in practice, instantaneous SNR values of underlying links are required at the transmitter and CSI is fed back from the relay and destination nodes to the source. Since FSO systems are full duplex, this feedback information can be easily sent over the reverse channel. The selected relay re-directs

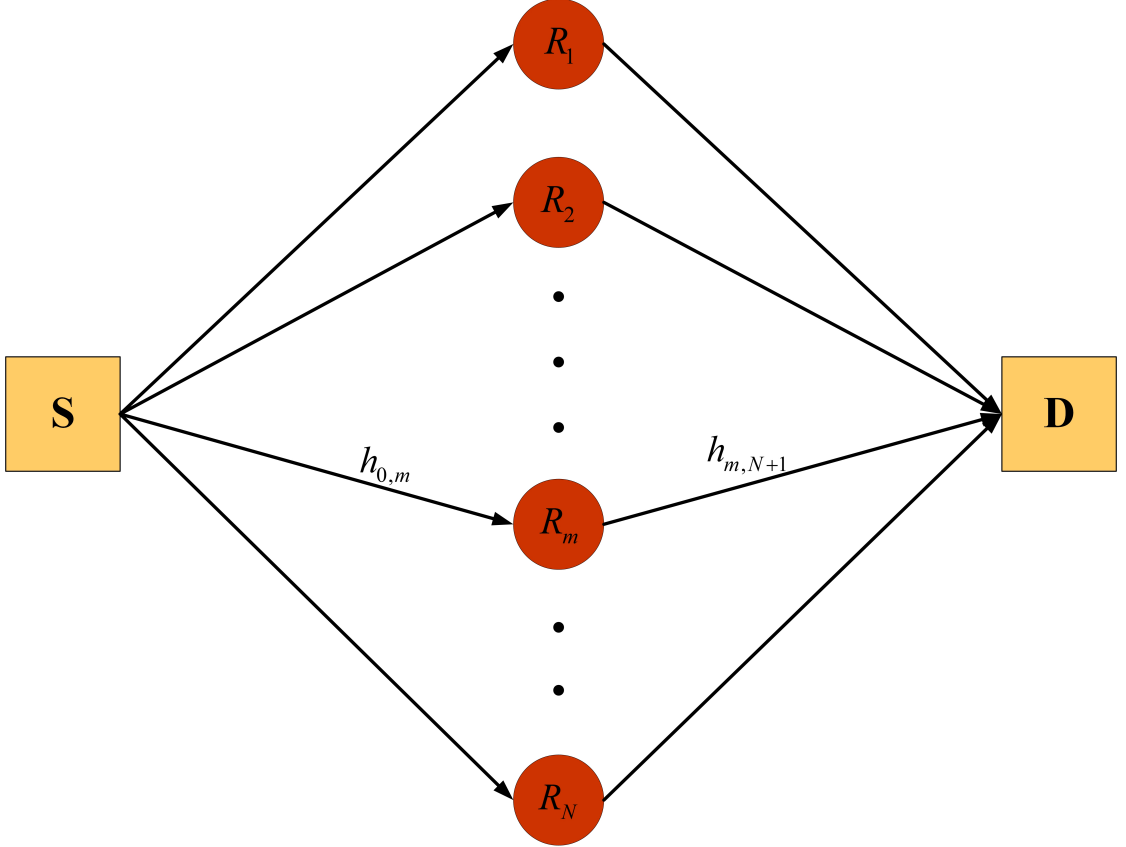


Figure 2: System model of a cooperative relaying system with N relays.

the optically amplified signal to the destination node.

Erbium-doped fiber amplifiers (EDFAs) are typically used at the destination to overcome the limitations of electrical noise. EDFA is a well-developed technology used in fiber-optic communication preamplifiers and in-line amplifiers in the 1550 nm range [50, 66]. They can be used as optical amplifier in relays in an atmospheric optical system along with other available devices for this wavelength band [67, 68]. Under the assumption of a high gain EDFA at the destination, we consider a shot-noise limited system in which the effect of thermal noise can be neglected and only shot noise caused by background radiation is dominant. Therefore, the noise at the destination is modeled by additive noise.

Following the transmission model in [49], assume that the source terminal transmits photons with rate $s(t)$, with an average of m_{si} , which obeys the Poisson distribution. Let $h_{0,i}$, $i = 1, 2, \dots, N$ denote the atmospheric turbulence fading for the link between the source and the i^{th} relay. Similarly, $h_{i,N+1}$ denotes the atmospheric turbulence fading for the link between the i^{th} relay and the destination. The received photon rate at the i^{th} relay is given by

$$r_i(t) = h_{0,i}s(t) + n_i(t) \quad (10)$$

where n_i is the background radiation for the link connecting the source to the i^{th} relay (S \rightarrow R _{i} channel). The photon count due to the background noise has Bose-Einstein distribution with an average of m_R which is assumed to be identical for all relay nodes.

The received photon rate at the destination from the i^{th} relay is

$$r_{N+1}^i(t) = h_{i,N+1}h_{0,i}G_i s(t) + h_{i,N+1}G_i n_i(t) + h_{i,N+1}n_i^{ASE}(t) + n_{i,N+1}(t) \quad (11)$$

where $n_{i,N+1}$ is the background radiation of the link between the i^{th} relay and the destination (R _{i} \rightarrow D channel). In (11), G_i is the gain of the i^{th} relay and its calculation depends on the degree of CSI availability (see Fig.3). In full-CSI relaying case, instantaneous CSI of the source-to-relay link is assumed to be available at the relay and is used for calculation of the amplification gain before retransmission of the received signal. On the other hand, in semi-blind relaying case, only statistical CSI (i.e., knowledge of the average fading power) is available; therefore a fixed coefficient is used in the amplification process.

In (11), n_i^{ASE} represents the ASE noise at the i^{th} relay and is modeled by an additive noise with the photon count of $m_i^{ASE} = n_{sp}(G_i - 1)$ and the DoF $M = 2B_o/B_e$ where B_o and B_e denote the equivalent optical and electrical bandwidth of optical filters respectively. DoF quantifies the ratio of optical filter bandwidth to the electrical bandwidth and can be on the order of 1000 unless narrowband optical filtering is

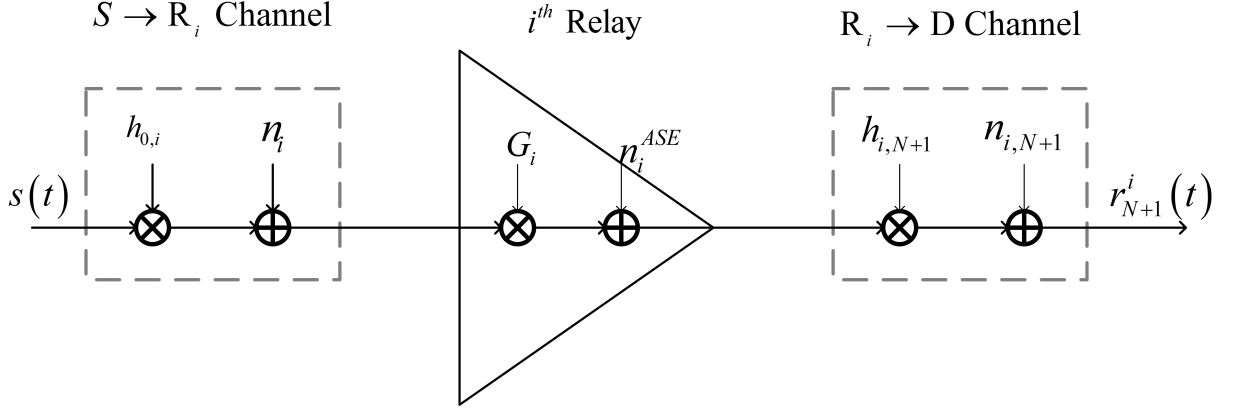


Figure 3: Mathematical model for transmission through one relay.

employed [51]. The factor n_{sp} denotes the spontaneous emission factor of the amplifier and can be approximately taken equal to unity for most practical purposes [49].

We assume a Gamma-Gamma distribution for atmospheric turbulence. Dropping the indexes i and j for notational simplicity, we have $h = h'I$ where h' is the path loss factor and I is the instantaneous irradiance whose distribution is given by 6. The instantaneous SNR is $\gamma = mh = \bar{\gamma}I$ with $\bar{\gamma} = mh'$ denoting the average SNR. Using 6 and a simple transformation, we can find the PDF of instantaneous SNR. The CDF of instantaneous SNR is further obtained as

$$F(\gamma) = \frac{(\alpha\beta)^{\frac{\alpha+\beta}{2}}}{\Gamma(\alpha)\Gamma(\beta)} \left(\frac{\gamma}{\bar{\gamma}}\right)^{\frac{(\alpha+\beta)}{2}} G_{2,1}^{1,3} \left[\alpha\beta \frac{\gamma}{\bar{\gamma}} \left| \begin{array}{c} 1 - \frac{\alpha+\beta}{2} \\ \frac{\alpha-\beta}{2}, \frac{\beta-\alpha}{2}, -\frac{\alpha+\beta}{2} \end{array} \right. \right] \quad (12)$$

where $G_{p,q}^{m,n}[\cdot]$ is the Meijer's G-function.

2.2 Outage Performance Analysis

The outage probability is defined as $P_{out} = \Pr(C(\gamma_T) < R_0)$, where R_0 is the target transmission rate and $C(\cdot)$ is the instantaneous capacity of the channel. Since capacity is a monotonically increasing function with respect to SNR, outage probability can be expressed as $P_{out} = \Pr(\gamma_T < \gamma_{th})$ where γ_T is the total SNR at the destination and

γ_{th} is the minimum acceptable end-to-end SNR.

The received photon rate at the destination from the i^{th} relay is given by (11). The photon count statistics at the destination obeys Laguerre distribution [69]. The probability of counts is given by

$$P_{count}(k) = Lag(k, a, b, M) = \frac{b^k}{(1+b)^{(k+m)}} \exp\left(-\frac{a}{1+b}\right) L_k^{M-1}\left(-\frac{a}{b(1+b)}\right) \quad (13)$$

where $L_k^M(x)$ is the generalized Laguerre polynomial of degree k , $a_i = G_i h_{0,i} h_{i,N+1} m_{s,i}$ and $b_i = m_R + G_i h_{i,N+1} m_R + h_{i,N+1} m_i^{ASE}$. Here, a_i and b_i are the average photon counts for the signal and the total background noise respectively. Therefore, we can write the end-to-end SNR through the i^{th} relaying path as

$$\gamma_{T_i} = \frac{a_i^2}{\sigma_{n_i}^2} \quad (14)$$

where $\sigma_{n_i}^2$ is the variance of the noise photon count at the receiver and is given by [51]

$$\sigma_{n_i}^2 = a_i + M b_i (1 + b_i) + 2 a_i b_i \quad (15)$$

In practice the average photon count due to background noise is much smaller than the photon count caused by ASE, so we have $b_i \approx h_{i,N+1} m_i^{ASE}$.

In full-CSI relaying scheme, the relay adjusts the gain of the amplifier at $G_i = m_{i,N+1}/h_{0,i} m_{0,i}$ while in semi-blind relaying the relay gain is fixed at $G_i = m_{i,N+1}/\bar{h}_{0,i} m_{0,i}$ [70]. Replacing (15) in (14) and using the definitions of G_i , we have

$$\gamma_{T_i}^{-1} = \begin{cases} \gamma_{i,N+1}^{-1} + M(\gamma_{0,i}^{-1} \gamma_{i,N+1}^{-1} + \gamma_{0,i}^{-2}) + 2\gamma_{0,i}^{-1}, \text{fullCSI} \\ \gamma_{0,i}^{-1} \gamma_{i,N+1}^{-1} \bar{\gamma}_{0,i} + M(\gamma_{0,i}^{-2} \gamma_{i,N+1}^{-1} \bar{\gamma}_{0,i} + \gamma_{0,i}^{-2}) + 2\gamma_{0,i}^{-1}, \text{Semi-blind} \end{cases} \quad (16)$$

where $\gamma_{0,i}$ and $\bar{\gamma}_{0,i}$ respectively denote instantaneous and average SNRs of $S \rightarrow R_i$ links. Similarly, and are respectively instantaneous and average SNRs of $R_i \rightarrow D$ links.

By using the max-min protocol metric defined in (9), we identify the best relay and obtain the total end-to-end SNR for the selected relay using (16). Replacing (16) in $P_{out} = \Pr(\gamma_T < \gamma_{th})$, we compute the outage probability numerically which will be presented in the following section.

2.3 Numerical Results and Discussions

We consider an FSO system with the optical wavelength of $\lambda = 1550$ nm. The source and the destination are located 3000 meters away from each other. We assume that the relays are placed at equal distances on the direct path linking the source to destination. Therefore, links are balanced and the average SNR is the same for all hops. We assume refractive index structure constant of $C_n^2 = 4.58 \times 10^{-13} \text{ m}^{-2/3}$ for each hop, an aperture with diameter of $D = 10$ mm threshold SNR of $\gamma_{th} = 15$ dB. The corresponding α and β parameters for the Gamma-Gamma distribution are calculated as 2.3 and 2.0 respectively.

In Fig.4, we present the outage performance of max-min protocol for $M = 1$ assuming full-CSI relaying. As a benchmark, we include the performance of a system where all relays participate in relaying phase (referred to as all-active protocol in [39]). Two protocols coincide for $N = 1$ and therefore achieve the same performance as expected. For $N = 2$, max-min protocol achieves the outage probability of 10^{-3} at SNR of 31.4 dB. This indicates a 0.7 dB improvement over all-active protocol which achieves the same performance at 32.1 dB. For higher values of N , the relative performance gain increases. At $N = 3$ and $N = 4$, the corresponding performance gains are obtained as 1.3 dB and 1.9 dB respectively.

In Fig.5, we present the outage performance of max-min protocol for DoF value $M = 1$ assuming semi-blind relaying. It is observed that additional performance improvements are obtained over full-CSI case. For $N = 2$, all-active protocol achieves the outage probability of 10^{-3} at SNR of 40.9 dB while max-min protocol reaches the same outage at 36.1 dB which represents a 4.8 dB improvement in performance. This indicates that using single relay becomes more effective in semi-blind relaying rather than full-CSI relaying.

In Fig.6, we present the outage performance for different values of DoF under the assumption of full-CSI relaying with four relays. For $M = 1$ (i.e., ideal case) all-active

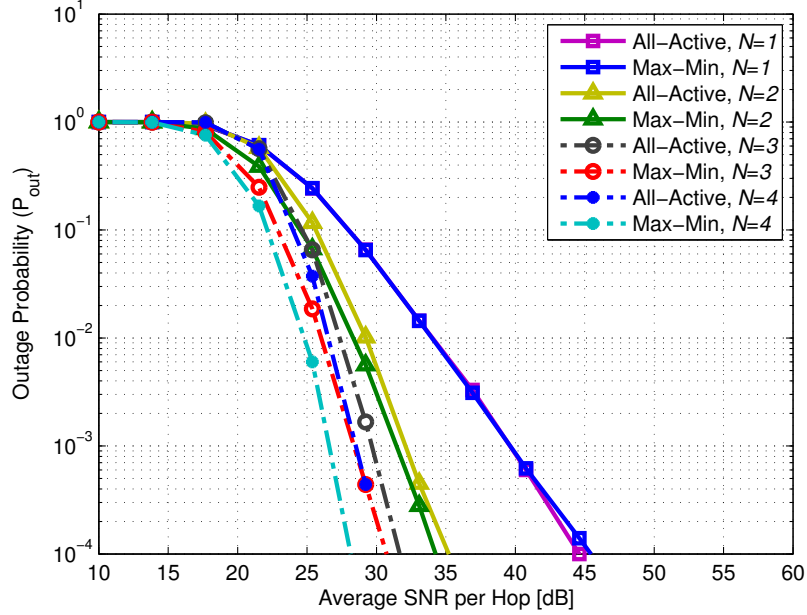


Figure 4: Outage probability of all-active and max-min protocol for full-CSI cooperative relaying system with different number of relays over Gamma-Gamma channels.

protocol achieves the outage probability of 10^{-3} at SNR of 28.5 dB while max-min protocol achieves the same performance at 26.6 dB. It shows 1.9 dB improvement in performance. The corresponding SNRs for $M = 10, 100$ and 1000 for all-active protocol are 29.1, 31.1 and 34.9 dB respectively. The max-min protocol achieves the same outage performance at SNR values of 27.2, 28.5 and 31.7 dB indicating performance improvements up to 3.2 dB.

In Fig.7, we present the outage performance for different values of DoF under the assumption of semi-blind relaying with four relays. For $M = 1$ max-min protocol has 11.2 dB improvement over all-active protocol. This slightly decreases to 10.2 and 9.3 dB for $M = 100$ and 1000, respectively.

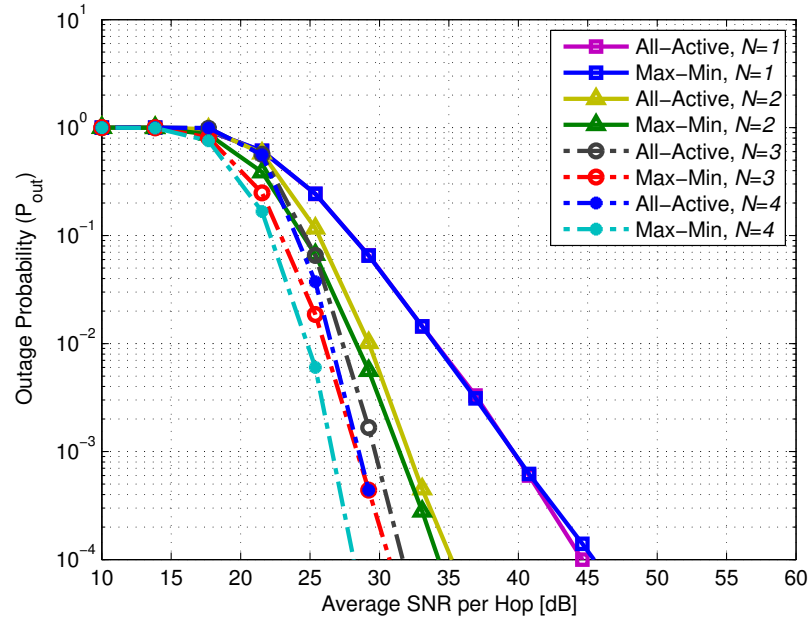


Figure 5: Outage probability of all-active and max-min protocol for semi-blind cooperative relaying system with different number of relays over Gamma-Gamma channels.

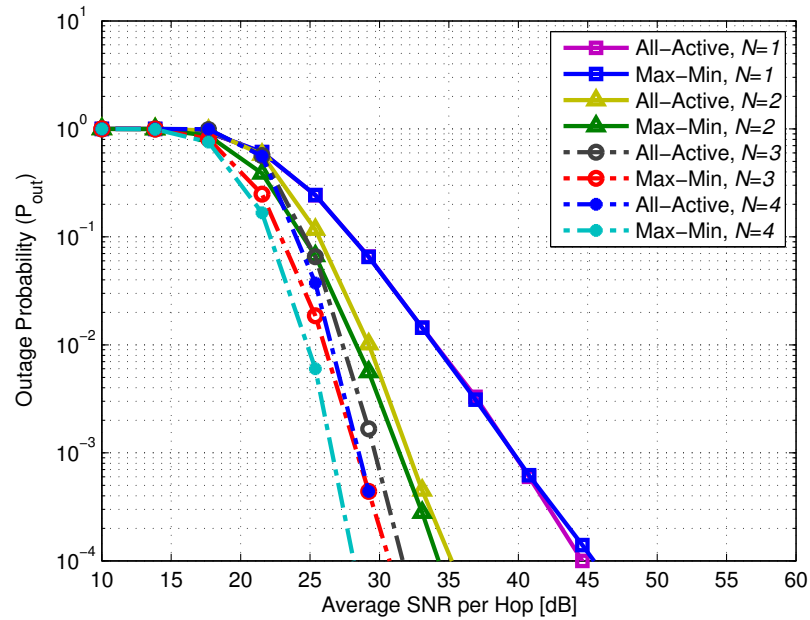


Figure 6: Outage probability of all-active and max-min protocol for full-CSI cooperative relaying system with different values of DoF over Gamma-Gamma channels.

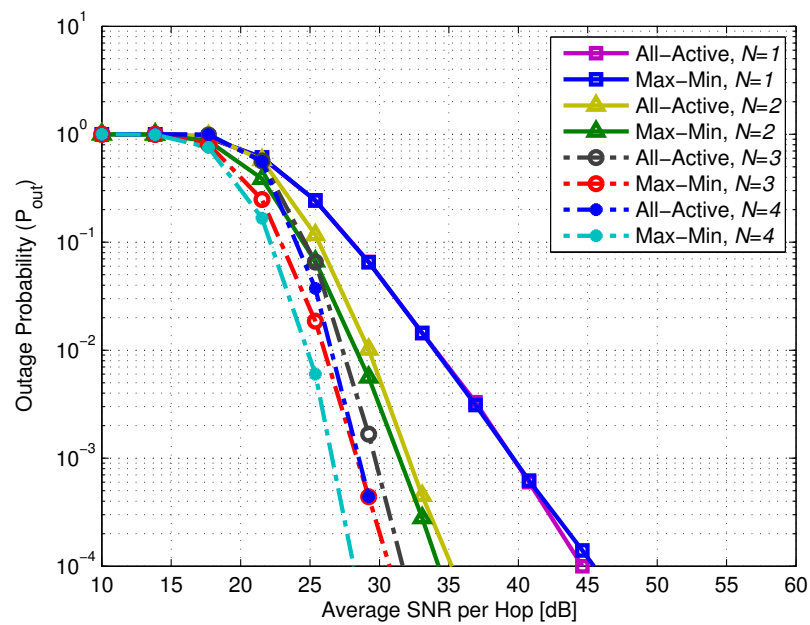


Figure 7: Outage probability of all-active and max-min protocol for semi-blind cooperative relaying system with different values of DoF over Gamma-Gamma channels.

CHAPTER III

RELAY-ASSISTED SPATIAL PULSE POSITION AMPLITUDE MODULATION IN FSO

In this chapter, we investigate the performance of SPPAM with multiple DF relays in which only relays that detects the signal correctly forward it to the destination. We derived a closed form for pairwise error probability (PEP) for the system under weak turbulence induced fading using which we present an upper bound for average bit error probability (BER).

The system under consideration has been depicted in Fig.8. We consider a relay-assisted FSO system with N DF relays located at the half distance between source and destination. We assume that source is equipped with N_t transmit antennas and destination has a single receive antenna ($N_r = 1$). Moreover, each relay has a single receive aperture to collect the received signal and one transmit aperture to send the data to the destination.

Source uses a SPPAM modulator to generate pulse position amplitude modulated (PPAM) signal vector $\mathbf{x}_{m,q}$ (which will be defined later) and send it to all N relays by a single active transmit antenna in transmission phase. In the relaying phase, relays which detect the signal vector and indices of active antenna in source correctly, forward this vector along with fading of corresponding channel to the destination.

SPPAM modulator in source divides the incoming bit stream into $\log_2(N_tMQ)$ bits. $\log_2(N_t)$ bits determine the indices of the active antenna in source during the transmission phase. $\log_2(M)$, and $\log_2(Q)$ bits respectively indicate the pulse position and amplitude in PPAM signal vector respectively (see Fig.9). The $M \times 1$

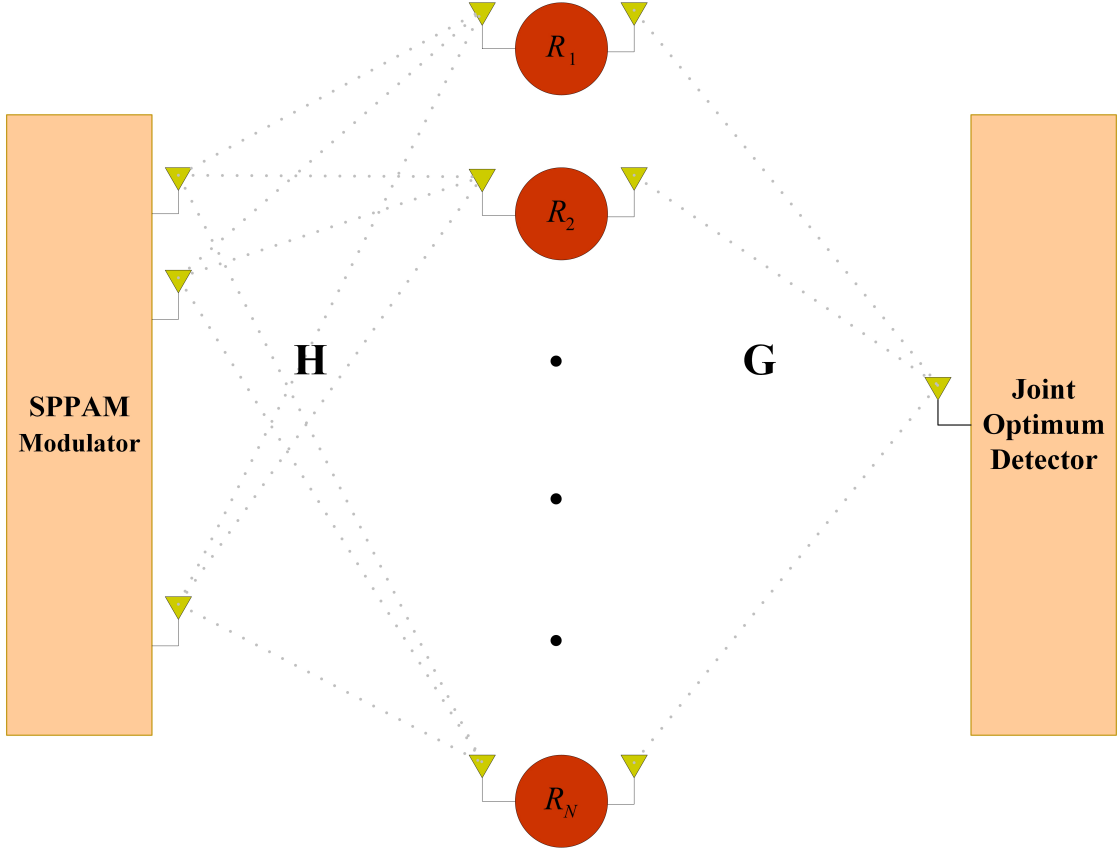


Figure 8: System with SPPAM in source and relays between source and destination.

dimensional PPAM signal vector $\mathbf{x}_{m,q}$ is given by

$$\mathbf{x}_{m,q} = [0 \dots 0 A_q 0 \dots 0]^T \quad (17)$$

where none zero element A_q is in m^{th} position and $1 \leq m \leq M$. $A_q = 2q\sqrt{M}/(Q+1)$, $1 \leq q \leq Q$ is the q^{th} level of amplitude in Q -ary PAM constellation. The spectral efficiency of SPPAM is $\log_2(N_t M Q)/M$, including the spectral efficiency of both PAM and PPM constellations [59].

In the first phase of transmission, the active antenna in source sends the signal vector to all the relays. The received noisy signal to the r^{th} relay from source when the j^{th} antenna is active can be written as

$$\mathbf{y}_{s,r} = p h_{r,j} \mathbf{x}_{m,q} + \mathbf{n}_{r,j} \quad (18)$$

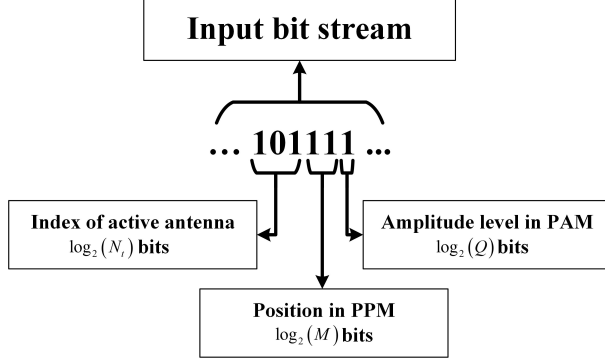


Figure 9: SPPAM mapping rule for system with $N_t = 8$, $M = 4$ and $Q = 2$.

where $h_{r,j} \triangleq [\mathbf{H}]_{rj}$ and $\mathbf{H}_{N \times N_t}$ is the channel gain matrix between source and the relays. $h \sim \ln(\mu_h, \sigma_h^2)$ is log-normal with parameters μ_h and σ_h^2 . $\mathbf{n}_{r,j}$ is the additive white Gaussian noise with zero mean and variance of $\sigma_n^2 I$. p is the average transmitted optical power per transmitter aperture which is related to the total transmitted power by $p = P_t/2N$.

In the second phase of transmission only the relays that correctly decoded the received signal transmit it to the destination. Let C denotes the decoding set which is a set of relays that are allowed to forward the signal. The signal received to the destination through the r^{th} relay ($r \in C$) can be represented as

$$\mathbf{y}_{r,d} = ph_{r,j}g_r\mathbf{x}_{m,q} + \mathbf{n}_{d,r} \quad (19)$$

where $g_r \triangleq [\mathbf{G}]_r$ and $\mathbf{G}_{N \times 1}$ is the channel gain matrix between relays and destination. $g \sim \ln(\mu_g, \sigma_g^2)$ is log-normal with parameters μ_g and σ_g^2 . $\mathbf{n}_{d,r}$ is the additive white Gaussian noise with zero mean and variance of $\sigma_n^2 I$.

We assume an aggregate channel model which considers both path loss effect and turbulence induced fading. Let h be the channel gain of a FSO link. We describe it as

$$h_{i,j} = |\alpha_{i,j}|^2 D_{i,j} \quad (20)$$

where $D_{i,j} = \text{loss}(d_{i,j})/\text{loss}(d_{s,d})$ is the normalized path loss for the link between

nodes i and j . $loss(d)$ is the path loss ratio for a FSO link with the length of d [22]

$$loss(d) = \frac{A_{TX}A_{RX}}{(\lambda d)^2} e^{-\sigma d} \quad (21)$$

where A_{TX} , A_{RX} , and λ are the transmitter aperture area, receiver aperture area and the optical wavelength respectively. σ is the attenuation coefficient which is depending on visibility [1, 8]. $|\alpha| = \exp(\chi)$ is the channel fading amplitude which has a log-normal distribution. The log-amplitude χ has a normal distribution with mean μ_χ and variance σ_χ^2 where $\mu_\chi = -\sigma_\chi^2$ to ensure that the fading does not attenuate or amplify the average optical power [20]. The log-amplitude variance depends on link distance, wave number k and refractive index structure constant C_n^2

$$\sigma_\chi^2 = 0.124k^{7/6}C_n^2d^{11/6} \quad (22)$$

We assume optimal maximum likelihood (ML) detector in relays with full channel state information (CSI) which jointly estimates the active antenna index \hat{j} in source and the transmitted signal vector $\mathbf{x}_{\hat{m}, \hat{q}}$ by minimizing the following metric

$$\left(\hat{j}, \hat{m}, \hat{q}\right) = \arg \min_{j, m, q} \left(\|\mathbf{y}_{s, r} - ph_{r, j}\mathbf{x}_{m, q}\|^2\right) \quad (23)$$

where $\mathbf{y}_{s, r}$ is the received signal to the r^{th} relay as described before.

We assume that K relays out of total N number relays detect the signal correctly. These relays forward the signal to the destination where there is an optimum MRC receiver that jointly estimates \hat{j} and $\mathbf{x}_{\hat{m}, \hat{q}}$ by minimizing the following metric

$$\left(\hat{j}, \hat{m}, \hat{q}\right) = \arg \min_{j, m, q} \left(\sum_{k=1}^K \|\mathbf{y}_{k, d} - ph_{k, j}g_k\mathbf{x}_{m, q}\|^2\right) \quad (24)$$

3.1 Performance Analysis

The exact average bit error probability (\overline{BER}) for SPPAM cannot be tracked easily however by using union bound technique [54, 71], an upper bound for \overline{BER} can be

given.

$$\overline{BER} \leq \frac{1}{2N_tMQ} \sum_{j=1}^{N_t} \sum_{\substack{\hat{j}=1 \\ \hat{j} \neq j}}^{N_t} \sum_{m=1}^M \sum_{\substack{\hat{m}=1 \\ \hat{m} \neq m}}^M \sum_{q=1}^Q \sum_{\substack{\hat{q}=1 \\ \hat{q} \neq q}}^Q \overline{PEP}_r \left(j, m, q, \hat{j}, \hat{m}, \hat{q} \mid h_{r,j}, h_{r,\hat{j}}, g_r, \mathbf{x}_{m,q}, \mathbf{x}_{\hat{m},\hat{q}} \right) \quad (25)$$

where \overline{PEP}_r is the average PEP for the link between source and destination including errors in relays and destination.

In order to better compute the upper bound for \overline{BER} , we determine different types of errors in relays and destination and find the corresponding \overline{PEP}_r expressions. The correct detection of active transmit antenna of source and PPAM signal vector at the receivers, introduces N_tMQ cases. The other cases are all in error which can be grouped into four different types of error based on the error detection in active transmit antenna or PPAM signal vector. This implies sixteen different types of errors in total. Here is the \overline{PEP}_r expression for the system when K relays detect the signal correctly

$$\begin{aligned} \overline{PEP}_r(e_1, e_2) &= \sum_{K=1}^N \binom{N}{K} (\overline{PEP}_{relay})^{N-K} (1 - \overline{PEP}_{relay})^K \\ &\quad \times \overline{PEP}_{MISO}, \quad I \leq e_1 \leq IV, I \leq e_2 \leq IV \end{aligned} \quad (26)$$

where e_1 , and e_2 are the different possible types of errors occurring in relays and destination respectively.

3.1.1 Calculating Average Pairwise Error Probability(\overline{PEP})

Assume $\eta = ph_{r,j}\mathbf{x}_{m,q}$ is the transmitted signal and $\hat{\eta} = ph_{r,\hat{j}}\mathbf{x}_{\hat{m},\hat{q}}$ is the received signal. $PEP(\eta \rightarrow \hat{\eta})$ is the probability of deciding on $\hat{\eta}$ when η has been transmitted.

The PEP for relays denoted by PEP_{relay} can be calculated as following:

$$\begin{aligned} PEP_{relay} &= PEP(\eta \rightarrow \hat{\eta}) = \Pr \left\{ \|\mathbf{y}_{s,r} - ph_{r,\hat{j}}\mathbf{x}_{\hat{m},\hat{q}}\|^2 < \|\mathbf{y}_{s,r} - ph_{r,j}\mathbf{x}_{m,q}\|^2 \right\} \\ &= \Pr \left\{ p^2 \|h_{r,j}\mathbf{x}_{m,q}\|^2 - p^2 \|h_{r,\hat{j}}\mathbf{x}_{\hat{m},\hat{q}}\|^2 + 2p (h_{r,\hat{j}}\mathbf{x}_{\hat{m},\hat{q}}^T - h_{r,j}\mathbf{x}_{m,q}^T) \mathbf{y}_{s,r} > 0 \right\} \quad (27) \\ &= \Pr \{U_r > 0\} \end{aligned}$$

After some manipulation it can be seen that U_r is a Gaussian random variable with mean $\mu_r = -p^2 \|h_{r,j} \mathbf{x}_{m,q} - h_{r,\hat{j}} \mathbf{x}_{\hat{m},\hat{q}}\|^2$ and variance of $\Sigma_r = 4\sigma_n^2 p^2 \|h_{r,j} \mathbf{x}_{m,q} - h_{r,\hat{j}} \mathbf{x}_{\hat{m},\hat{q}}\|^2$.

We can find the average PEP for relays as following:

$$\begin{aligned} \overline{PEP}_{relay} &= E \left\{ Q \left(\sqrt{\frac{p^2}{4\sigma_n^2} \|h_{r,j} \mathbf{x}_{m,q} - h_{r,\hat{j}} \mathbf{x}_{\hat{m},\hat{q}}\|^2} \right) \right\} \\ &= E \left\{ Q \left(\sqrt{\frac{\rho}{4} \Omega_1} \right) \right\} \end{aligned} \quad (28)$$

where $\rho = p^2/\sigma_n^2$ is the electrical SNR and $\Omega_1 = \|h_{r,j} \mathbf{x}_{m,q} - h_{r,\hat{j}} \mathbf{x}_{\hat{m},\hat{q}}\|^2$ is the error metric in relays.

With similar procedure we can find the average PEP expression in the destination when K relays out of N relays are in the decoding set.

$$\begin{aligned} \overline{PEP}_{MISO} &= E \left\{ Q \left(\sqrt{\frac{\rho}{4} \sum_{k=1}^K g_k^2 \|h_{k,j} \mathbf{x}_{m,q} - h_{k,\hat{j}} \mathbf{x}_{\hat{m},\hat{q}}\|^2} \right) \right\} \\ &= E \left\{ Q \left(\sqrt{\frac{\rho}{4} \Omega_2} \right) \right\} \end{aligned} \quad (29)$$

where ρ is as defined before and $\Omega_2 = \sum_{k=1}^K g_k^2 \|h_{k,j} \mathbf{x}_{m,q} - h_{k,\hat{j}} \mathbf{x}_{\hat{m},\hat{q}}\|^2$ is the error metric in destination.

It should be noted that expected value of Q function can be calculated using Craigs formulation [72].

$$Q(x) = \frac{1}{\pi} \int_0^{\pi/2} \exp\left(-\frac{x^2}{2\sin^2\theta}\right) d\theta \quad (30)$$

We drop the indexes for simplicity and use 30 to find 28 and 29.

$$\begin{aligned} \overline{PEP} &= E \left\{ Q \left(\sqrt{\frac{\rho}{4} \Omega} \right) \right\} \\ &= \frac{1}{\pi} \int_0^{\pi/2} \int_{\Omega} \exp\left(-\frac{\rho\Omega}{8\sin^2\theta}\right) f_{\Omega}(\Omega) d\Omega d\theta \\ &= \frac{1}{\pi} \int_0^{\pi/2} M_{\Omega} \left(-\frac{\rho\Omega}{8\sin^2\theta} \right) d\theta \end{aligned} \quad (31)$$

where $M_{\Omega}(t) = \int_0^{\infty} f_{\Omega}(\Omega) e^{\Omega t} d\Omega$ is the moment generating function (MGF) of random variable Ω .

3.1.2 Defining Error Types

As we mentioned before there are four different types of errors for relays and destination (terminals) which we will define in the following.

Type I: The index of the active transmit antenna and the pulse position has been detected correctly but the pulse amplitude has not, i.e. $j = \hat{j}$, $m = \hat{m}$ and $q \neq \hat{q}$. The error metrics corresponding to this type of errors for relays and destination are

$$\Omega_1^I = (A_q - A_{\hat{q}})^2 h_{r,j}^2 \quad (32)$$

$$\Omega_2^I = \sum_{k=1}^K (A_q - A_{\hat{q}})^2 g_k^2 h_{k,j}^2 \quad (33)$$

There are $N_t M Q (Q - 1)$ terms corresponding to this type of error for terminals.

Type II: The index of the active transmit antenna has been detected correctly but the pulse position has not, i.e $j \neq \hat{j}$, and $m \neq \hat{m}$. The error metrics for this type of error are

$$\Omega_1^{II} = (A_q^2 + A_{\hat{q}}^2) h_{r,j}^2 \quad (34)$$

$$\Omega_2^{II} = \sum_{k=1}^K (A_q^2 - A_{\hat{q}}^2) g_k^2 h_{k,j}^2 \quad (35)$$

There are $N_t M (M - 1) Q^2$ terms corresponding to this type of error for relays and also for destination.

Type III: Neither the index of the active transmit antenna nor the pulse position has been detected correctly, i.e $j \neq \hat{j}$, and $m \neq \hat{m}$. The error metrics of this type of error can be represented as

$$\Omega_1^{III} = A_q^2 h_{r,j}^2 + A_{\hat{q}}^2 h_{r,\hat{j}}^2 \quad (36)$$

$$\Omega_2^{III} = \sum_{k=1}^K (A_q^2 h_{k,j}^2 + A_{\hat{q}}^2 h_{k,\hat{j}}^2) g_k^2 \quad (37)$$

There are $N_t (N_t - 1) M (M - 1) Q^2$ terms corresponding to this type of error.

Type IV: The pulse position has been detected correctly but the index of active transmit antenna has not, i.e $j \neq \hat{j}$, and $m = \hat{m}$. The error metrics corresponding to this type of error is as following:

$$\Omega_1^{IV} = (A_q h_{r,j} - A_{\hat{q}} h_{r,\hat{j}})^2 \quad (38)$$

$$\Omega_2^{IV} = \sum_{k=1}^K (A_q h_{k,j} - A_{\hat{q}} h_{k,\hat{j}})^2 g_k^2 \quad (39)$$

There are $N_t(N_t - 1)MQ^2$ terms corresponding to this type of error.

It should be mentioned that except for the first type of errors, for the other ones whether the pulse amplitude has been detected correctly or not does not affect the statistical description of error metrics.

In order to use (31) to find \overline{PEP} we should find the MGF of the random variable Ω for all the above cases. It should be noted that error types *I*, *II* and *III* are weighted sum of squared log-normal random variables. It can be shown that the sum of log-normal random variables whether they are correlated or not can be approximated by a single log-normal random variable [10, 73].

Lets assume that $X_i \sim N(\mu_X, \sigma_X^2)$ and $1 \leq i \leq N$, are i.i.d normal random variables with mean μ_X and variance σ_X^2 . Then $Y_i = e^{X_i}$ are i.i.d log-normal random variables. Lets assume that $S = \sum_{i=1}^N c_i Y_i$ is a random variable with $E[S] = m_S$, and $Var[S] = v_S^2$. It can be approximated by $S \approx e^U$, a log-normal random variable with parameters μ_U and σ_U^2 and $U \sim N(\mu_U, \sigma_U^2)$ is a normal random variable with mean $\mu_U = \ln\left(m_S / \sqrt{1 + v_S^2/m_S^2}\right)$ and variance $\sigma_U^2 = \ln\left(1 + v_S^2/m_S^2\right)$.

Using Gauss-Hermite integration we can approximate the MGF function of as following [73].

$$M_S(t) \approx \sum_{n=1}^{N_e} \frac{\omega_n}{\sqrt{\pi}} \exp\left(t \exp\left(\sqrt{2}\sigma_U a_n + \mu_U\right)\right) \quad (40)$$

where ω_n and a_n are weights and abscissas of Gauss-Hermite integration given in [74].

We can use formula (40) as MGF function needed in (31) to find \overline{PEP} for different

types of errors.

$$\begin{aligned}
\overline{PEP} &= \frac{1}{\pi} \int_0^{\pi/2} M_S \left(-\frac{\rho S}{8 \sin^2 \theta} \right) d\theta \\
&\approx \frac{1}{\pi} \int_0^{\pi/2} \sum_{n=1}^{N_e} \frac{\omega_n}{\sqrt{\pi}} \exp \left(-\frac{\rho S}{8 \sin^2 \theta} \exp \left(\sqrt{2} \sigma_U a_n + \mu_U \right) \right) d\theta \\
&\approx \sum_{n=1}^{N_e} \frac{\omega_n}{\sqrt{\pi}} Q \left(\sqrt{\frac{\rho}{4}} \exp \left(\sqrt{2} \sigma_U a_n + \mu_U \right) \right)
\end{aligned} \tag{41}$$

The goal here is to find the mean and variance of approximated log-normal random variable for the first three error types. It should be noted that the fourth type is the difference of two log-normal random variable which cannot be approximated by a log-normal distribution.

For type *I* and *II* we have

$$m_{\Omega_1} = c \exp \left(2\mu_h + 2\sigma_h^2 \right) \tag{42}$$

$$v_{\Omega_1}^2 = c^2 \left(\exp \left(4\sigma_h^2 \right) - 1 \right) \exp \left(4\mu_h + 4\sigma_h^2 \right) \tag{43}$$

$$m_{\Omega_2} = K c \exp \left(2 \left(\mu_h + \mu_g \right) + 2 \left(\sigma_h^2 + \sigma_g^2 \right) \right) \tag{44}$$

$$v_{\Omega_2}^2 = K c^2 \left(\exp \left(4 \left(\sigma_h^2 + \sigma_g^2 \right) \right) - 1 \right) \exp \left(4 \left(\mu_h + \mu_g \right) + 4 \left(\sigma_h^2 + \sigma_g^2 \right) \right) \tag{45}$$

where $c = (A_q - A_{\hat{q}})^2$ and $c = (A_q + A_{\hat{q}})^2$ for error types *I* and *II* respectively. For type *III* we have

$$m_{\Omega_1} = (c_1 + c_2) \exp \left(2\mu_h + 2\sigma_h^2 \right) \tag{46}$$

$$v_{\Omega_1}^2 = (c_1^2 + c_2^2) \left(\exp \left(4\sigma_h^2 \right) - 1 \right) \exp \left(4\mu_h + 4\sigma_h^2 \right) \tag{47}$$

$$m_{\Omega_2} = K (c_1 + c_2) \left(2 \left(\mu_h + \mu_g \right) + 2 \left(\sigma_h^2 + \sigma_g^2 \right) \right) \tag{48}$$

$$v_{\Omega_2}^2 = K (c_1^2 + c_2^2) \left(\exp \left(4 \left(\sigma_h^2 + \sigma_g^2 \right) \right) - 1 \right) \exp \left(4 \left(\mu_h + \mu_g \right) + 4 \left(\sigma_h^2 + \sigma_g^2 \right) \right) \tag{49}$$

where $c_1 = A_q^2$ and $c_2 = A_{\hat{q}}^2$. It should be mentioned that μ_h and σ_h^2 are the channel gain parameters for the link between source and relays and μ_g and σ_g^2 are the channel gain parameters for the link between relays and destination.

Using all the information above, we can find upper bound for \overline{BER} as following

$$\overline{BER} \leq \sum_{e_1=I}^{IV} \sum_{e_2=I}^{IV} T(e_1, e_2) \quad (50)$$

where

$$T(I, I) = \frac{N_t M}{2L} \sum_{q_1=1}^Q \sum_{\substack{\hat{q}_1=1 \\ \hat{q}_1 \neq q_1}}^Q \sum_{q_2=1}^Q \sum_{\substack{\hat{q}_2=1 \\ \hat{q}_2 \neq q_2}}^Q \overline{PEP}_r(I, I) \quad (51)$$

$$T(I, II) = \frac{N_t M (M-1)}{2L} \sum_{q_1=1}^Q \sum_{\substack{\hat{q}_1=1 \\ \hat{q}_1 \neq q_1}}^Q \sum_{q_2=1}^Q \sum_{\hat{q}_2=1}^Q \overline{PEP}_r(I, II) \quad (52)$$

$$T(I, III) = \frac{N_t (N_t - 1) M (M-1)}{2L} \sum_{q_1=1}^Q \sum_{\substack{\hat{q}_1=1 \\ \hat{q}_1 \neq q_1}}^Q \sum_{q_2=1}^Q \sum_{\hat{q}_2=1}^Q \overline{PEP}_r(I, III) \quad (53)$$

$$T(I, IV) = \frac{N_t (N_t - 1) M}{2L} \sum_{q_1=1}^Q \sum_{\substack{\hat{q}_1=1 \\ \hat{q}_1 \neq q_1}}^Q \sum_{q_2=1}^Q \sum_{\hat{q}_2=1}^Q \overline{PEP}_r(I, IV) \quad (54)$$

$$T(II, I) = \frac{N_t M (M-1)}{2L} \sum_{q_1=1}^Q \sum_{\hat{q}_1=1}^Q \sum_{q_2=1}^Q \sum_{\substack{\hat{q}_2=1 \\ \hat{q}_2 \neq q_2}}^Q \overline{PEP}_r(II, I) \quad (55)$$

$$T(II, II) = \frac{N_t M (M-1)^2}{2L} \sum_{q_1=1}^Q \sum_{\hat{q}_1=1}^Q \sum_{q_2=1}^Q \sum_{\hat{q}_2=1}^Q \overline{PEP}_r(II, II) \quad (56)$$

$$T(II, III) = \frac{N_t (N_t - 1) M (M-1)^2}{2L} \sum_{q_1=1}^Q \sum_{\hat{q}_1=1}^Q \sum_{q_2=1}^Q \sum_{\hat{q}_2=1}^Q \overline{PEP}_r(II, III) \quad (57)$$

$$T(II, IV) = \frac{N_t (N_t - 1) M (M-1)}{2L} \sum_{q_1=1}^Q \sum_{\hat{q}_1=1}^Q \sum_{q_2=1}^Q \sum_{\hat{q}_2=1}^Q \overline{PEP}_r(II, IV) \quad (58)$$

$$T(III, I) = \frac{N_t (N_t - 1) M (M-1)}{2L} \sum_{q_1=1}^Q \sum_{\hat{q}_1=1}^Q \sum_{q_2=1}^Q \sum_{\substack{\hat{q}_2=1 \\ \hat{q}_2 \neq q_2}}^Q \overline{PEP}_r(III, I) \quad (59)$$

$$T(III, II) = \frac{N_t (N_t - 1) M (M-1)^2}{2L} \sum_{q_1=1}^Q \sum_{\hat{q}_1=1}^Q \sum_{q_2=1}^Q \sum_{\hat{q}_2=1}^Q \overline{PEP}_r(III, II) \quad (60)$$

$$T(III, III) = \frac{N_t (N_t - 1)^2 M (M-1)^2}{2L} \sum_{q_1=1}^Q \sum_{\hat{q}_1=1}^Q \sum_{q_2=1}^Q \sum_{\hat{q}_2=1}^Q \overline{PEP}_r(III, III) \quad (61)$$

$$T(III, IV) = \frac{N_t(N_t - 1)^2 M(M - 1)}{2L} \sum_{q_1=1}^Q \sum_{\hat{q}_1=1}^Q \sum_{q_2=1}^Q \sum_{\hat{q}_2=1}^Q \overline{PEP}_r(III, IV) \quad (62)$$

$$T(IV, I) = \frac{N_t(N_t - 1) M}{2L} \sum_{q_1=1}^Q \sum_{\hat{q}_1=1}^Q \sum_{q_2=1}^Q \sum_{\substack{\hat{q}_2=1 \\ \hat{q}_2 \neq q_2}}^Q \overline{PEP}_r(IV, I) \quad (63)$$

$$T(IV, II) = \frac{N_t(N_t - 1) M(M - 1)}{2L} \sum_{q_1=1}^Q \sum_{\hat{q}_1=1}^Q \sum_{q_2=1}^Q \sum_{\hat{q}_2=1}^Q \overline{PEP}_r(IV, II) \quad (64)$$

$$T(IV, III) = \frac{N_t(N_t - 1)^2 M(M - 1)}{2L} \sum_{q_1=1}^Q \sum_{\hat{q}_1=1}^Q \sum_{q_2=1}^Q \sum_{\hat{q}_2=1}^Q \overline{PEP}_r(IV, III) \quad (65)$$

$$T(IV, IV) = \frac{N_t(N_t - 1)^2 M}{2L} \sum_{q_1=1}^Q \sum_{\hat{q}_1=1}^Q \sum_{q_2=1}^Q \sum_{\hat{q}_2=1}^Q \overline{PEP}_r(IV, IV) \quad (66)$$

3.2 Numerical Results and Discussions

We consider a FSO system with the optical wavelength of $\lambda = 1550$ nm. The source and the destination are located at distance of $L = 500$ m from each other and relays are in the half distance between source and destination. We assumed refractive index of $C_n^2 = 10^{-14} \text{ m}^{-2/3}$ for weak turbulence fading channels and visibility of 0.43 dB/km (i.e., $\sigma \approx 0.1$).

In this section we present the simulation result for error performance of SPPAM modulation for different configurations and different number of relays. In all the simulations we assumed one receiver antenna in each terminal (relays and destination) and we used Gray mapping for bit to symbol conversion. Finally we used (50) to find the upper bound for BER of each configuration.

In Fig.10, we present the average BER of a SPPAM system with $N_t = 4$, $M = 2$, and $Q = 2$ for one and four number of parallel relays in the middle of source and destination. As a benchmark we included the performance of point to point transmission with the same configuration. It can be seen that even though using only one relay does not affect the performance strongly, increasing the number of relays improves the performance of system significantly. The system with one relay achieves

the bit error rate of 10^{-2} at SNR of more than 40 dB while the same performance achieved by system with four relays at 16.7 dB. This shows performance gain of more than 23 dB. Also the upper bound is tighter when we increase the number of relays.

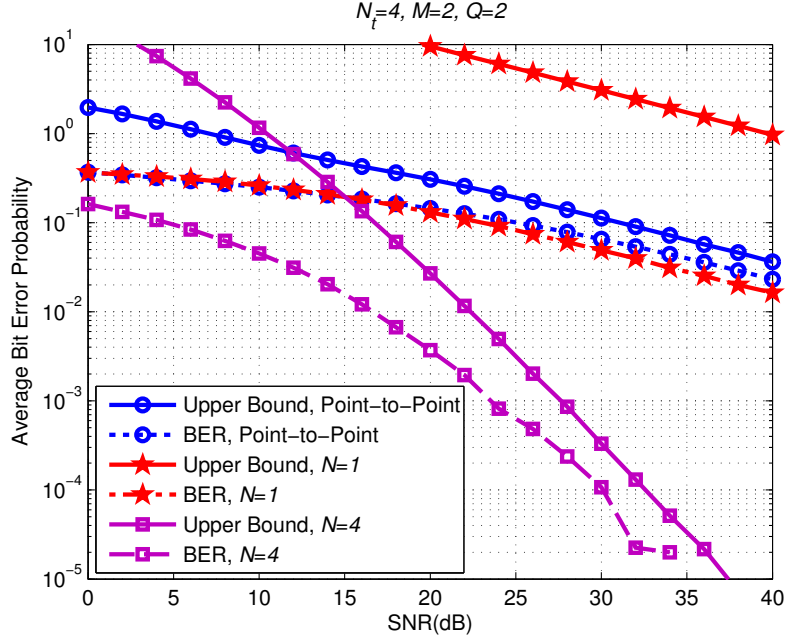


Figure 10: Average BER of a system with SPPAM in source and different number of relays over log-normal channels.

In Fig.11, we present the performance of two different system configurations both with the same spectral efficiency. One is the conventional SSK with 8 number of transmit antenna in source which means 3 bits per symbol and spectral efficiency of 3 bits/s/Hz. The other one is a SPPAM system with $N_t = 4, M = 1$ and $Q = 2$ with the same rate and same spectral efficiency. In both configurations we assumed $N = 3$ number of relays between source and destination. The conventional SSK achieves the performance of 10^{-3} at 36.5 dB while the same performance achieves by SPPAM at 30.7 dB. This shows 5.8 dB performance gain for system with SPPAM over conventional SSK.

In Fig.12, we compare the performance of three systems, all of which has $N_t = 4$ number of transmit antennas but different spectral efficiencies, for both point to pint

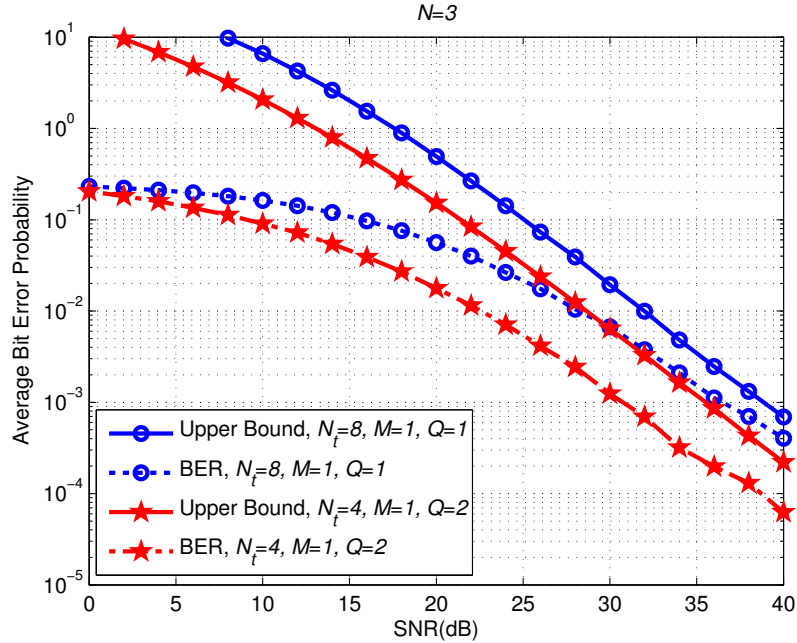


Figure 11: Average BER of systems with $N = 4$ relays and spectral efficiency of 3 bits/s/Hz with different number of transmit antennas in source over log-normal channels.

and relay assisted communication with $N = 4$ number of relays. It can be seen that system with $M = 2$ and $Q = 1$ which result in spectral efficiency of 1.5 bits/s/Hz achieves the bit error rate of 10^{-3} in SNR of 21.9 dB. This is better than systems with $M = 2$ and $Q = 2$ with spectral efficiency of 2 bits/s/Hz and $M = 1$ and $Q = 2$ with spectral efficiency of 3 bits/s/Hz which reaches the same performance in SNR of 23.5 dB and 26.2 dB respectively. It can be seen that there is trade-off between bit error rate and spectral efficiency of systems with SPPAM and relays, however this trade-off is not very effective in point to point communication.

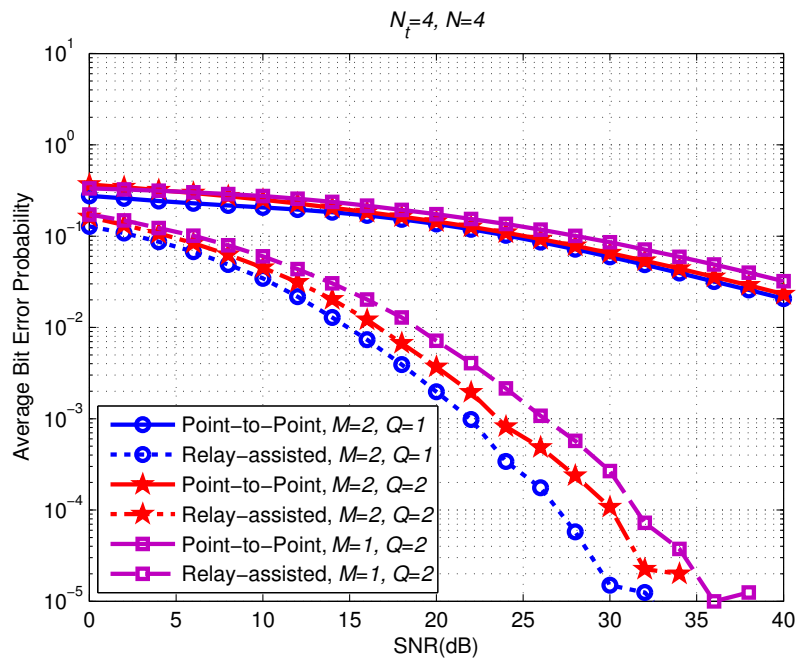


Figure 12: Average BER of systems with $N = 4$ relays and spectral efficiency of 3 bits/s/Hz with different number of transmit antennas in source over log-normal channels.

CHAPTER IV

CONCLUSIONS AND FUTURE DIRECTIONS

Despite the major advantage of FSO communication such as high data rate, unregulated spectrum and high security, its performance is severely degraded by the atmospheric turbulence induced fading, particularly in long-range link distances. Relay assisted systems has been introduced in literature to extend the range and mitigate the effects of turbulence induced fading in FSO links. Increasing the speed and spectral efficiency of optical systems is another major concern that has been addressed in literature. This thesis has addressed the performance analysis of relay assisted free space communication with different system configurations.

In chapter 2, we have investigated the outage performance of IM/DD FSO systems with number of All-optical AF relays between source and destination and we used max-min relay selection protocol to find the best relay. Unlike conventional relay assisted systems all-optical relays processed the signals in optical domain and avoid the OE and EO conversion which allows increasing the speed of system. Based on photon counting approach we have presented the outage performance over Gamma-Gamma turbulence channels for full-CSI and semi-blind relays. Numerical results have demonstrated that relay selection brings significant performance improvements over all-active protocol. Up to 11.2 dB improvements were obtained for a system with four relays. Here we selected the first best relay; however employing a protocol to choose the second best relay or in general n^{th} best relay when the first best one is not available can be investigate as a future work.

In chapter 3, we have focused our attention to increase the spectral efficiency of

FSO system while improving the error performance by using relay assisted communication along with spatial modulation. We investigated the error performance of a FSO system with SPPAM in source and multiple parallel DF relays in the half distance between source and destination. We presented the upper bound for average bit error rate of system over log-normal turbulence channels for systems with several numbers of relays and transmit antennas in source. Numerical results demonstrate a significant performance improvement for system with relays over point to point communications. Over 25 dB improvement has been achieved by a system with four relays. Here we assumed that all the relays that detect the signal correctly send it to the destination simultaneously and there is no relay selection. Therefore, a possible research subject could be employing protocols to choose the first best relay or in general n^{th} best relay when the first best one is not available. Furthermore, this analysis can be extended to system with more than one receiver aperture in the destination which will obtain diversity gain. Moreover, using relays for performing spatial modulation instead of simply relaying the signal to destination is another interesting topic that can be investigated.

Bibliography

- [1] S. Arnon, J. Barry, G. Karagiannidis, R. Schober, and M. Uysal, *Advanced Optical Wireless Communication Systems*. New York: Cambridge University Press, 2012.
- [2] R. Gagliardi and S. Karp, *Optical Communications*. New York, USA: Wiley, 1995.
- [3] H. Hemmati, *Near-Earth Laser Communications*. USA: Taylor & Francis, 2014.
- [4] H. Willebrand and B. Ghuman, *Free Space Optics: Enabling Optical Connectivity in Today's Networks*. USA: Sams, 2002.
- [5] L. Andrews, R. Phillips, and C. Hopon, *Laser Beam Scintillation with Applications*. Washington, USA: SPIE Press, 2001.
- [6] M. Karimi and M. Nasiri-Kenari, "BER analysis of cooperative systems in free-space optical networks," *J. Lightw. Technol.*, vol. 27, no. 24, pp. 5639–5647, 2009.
- [7] D. Kedar and S. Arnon, "Urban optical wireless communication networks: the main challenges and possible solutions," *IEEE Commun. Mag.*, vol. 42, no. 5, pp. S2–S7, 2004.
- [8] L. Andrews and R. Phillips, *Laser Beam Propagation Through Random Media*. Washington, USA: SPIE Press, 2nd ed., 2005.
- [9] S. Arnon, "Optimization of urban optical wireless communication systems," *IEEE Trans. Wireless Commun.*, vol. 2, no. 4, pp. 626–629, 2003.
- [10] S. M. Navidpour, M. Uysal, and M. Kavehrad, "BER performance of free-space optical transmission with spatial diversity," *IEEE Trans. Wireless Commun.*, vol. 6, no. 8, pp. 2813–2819, 2007.
- [11] E. Bayaki, R. Schober, and R. K. Mallik, "Performance analysis of MIMO free-space optical systems in gamma-gamma fading," *IEEE Trans. Commun.*, vol. 57, no. 11, pp. 3415–3424, 2009.
- [12] Z. Xiaoming and J. M. Kahn, "Free-space optical communication through atmospheric turbulence channels," *IEEE Trans. Commun.*, vol. 50, no. 8, pp. 1293–1300, 2002.
- [13] N. Das, *Optical Communication: In Tech*. Croatia: In Tech, 2012.
- [14] R. S. Lawrence and J. W. Strohbehm, "A survey of clear-air propagation effects relevant to optical communications," *Proc. IEEE*, vol. 58, no. 10, pp. 1523–1545, 1970.

- [15] S. Karp, *Optical channels: fibers, clouds, water, and the atmosphere*. Plenum Press, 1988.
- [16] E. Biglieri, J. Proakis, and S. Shamai, “Fading channels: information-theoretic and communications aspects,” *IEEE Trans. Inf. Theory*, vol. 44, no. 6, pp. 2619–2692, 1998.
- [17] L. C. Andrews, R. L. Phillips, C. Y. Hopen, and M. A. Al-Habash, “Theory of optical scintillation,” *J. Opt. Soc. Am. A.*, vol. 16, no. 6, pp. 1417–1429, 1999.
- [18] M. A. Al-Habash, R. L. Phillips, and L. C. Andrews, “Mathematical model for the irradiance probability density function of a laser beam propagating through turbulent media,” *OSA J. Opt. Eng.*, vol. 40, no. 8, pp. 1554–1562, 2001.
- [19] Z. Xiaoming and J. M. Kahn, “Performance bounds for coded free-space optical communications through atmospheric turbulence channels,” *IEEE Trans. Wireless Commun.*, vol. 51, no. 8, pp. 1233–1239, 2003.
- [20] M. Uysal, S. M. Navidpour, and L. Jing, “Error rate performance of coded free-space optical links over strong turbulence channels,” *IEEE Commun. Lett.*, vol. 8, no. 10, pp. 635–637, 2004.
- [21] Z. Xiaoming and J. M. Kahn, “Markov chain model in maximum-likelihood sequence detection for free-space optical communication through atmospheric turbulence channels,” *IEEE Trans. Commun.*, vol. 51, no. 3, pp. 509–516, 2003.
- [22] S. M. Haas, *Capacity of and coding for multiple-aperture, wireless, optical communications*. Thesis, 2003.
- [23] E. J. Lee and V. W. S. Chan, “Part 1: optical communication over the clear turbulent atmospheric channel using diversity,” *IEEE J. Sel. Areas Commun.*, vol. 22, no. 9, pp. 1896–1906, 2004.
- [24] A. A. Farid and S. Hranilovic, “Diversity gain and outage probability for MIMO free-space optical links with misalignment,” *IEEE Trans. Commun.*, vol. 60, no. 2, pp. 479–487, 2012.
- [25] M. Safari and M. Uysal, “Relay-assisted free-space optical communication,” *IEEE Trans. Wireless Commun.*, vol. 7, no. 12, pp. 5441–5449, 2008.
- [26] C. Abou-Rjeily and A. Slim, “Cooperative diversity for free-space optical communications: Transceiver design and performance analysis,” *IEEE Trans. Commun.*, vol. 59, no. 3, pp. 658–663, 2011.
- [27] Z. Xiaoming, J. M. Kahn, and W. Jin, “Mitigation of turbulence-induced scintillation noise in free-space optical links using temporal-domain detection techniques,” *IEEE Photon. Technol. Lett.*, vol. 15, no. 4, pp. 623–625, 2003.

- [28] S. G. Wilson, M. Brandt-Pearce, C. Qianling, and M. Baedke, "Optical repetition MIMO transmission with multipulse PPM," *IEEE J. Sel. Areas Commun.*, vol. 23, no. 9, pp. 1901–1910, 2005.
- [29] S. M. Navidpour, M. Uysal, and L. Jing, "BER performance of MIMO free-space optical links," in *IEEE Vehicular Technology Conference (VTC)*, vol. 5, pp. 3378–3382 Vol. 5.
- [30] A. Garcia-Zambrana, C. Castillo-Vazquez, B. Castillo-Vazquez, and A. Hiniesta-Gomez, "Selection transmit diversity for FSO links over strong atmospheric turbulence channels," *IEEE Photon. Technol. Lett.*, vol. 21, no. 14, pp. 1017–1019, 2009.
- [31] C. Abou-Rjeily, "On the optimality of the selection transmit diversity for MIMO-FSO links with feedback," *IEEE Commun. Lett.*, vol. 15, no. 6, pp. 641–643, 2011.
- [32] M. A. Khalighi and M. Uysal, "Survey on free space optical communication: A communication theory perspective," *IEEE Commun. Surveys Tuts.*, vol. PP, no. 99, pp. 1–1, 2014.
- [33] A. J. Paulraj, D. A. Gore, R. U. Nabar, and H. Bolcskei, "An overview of MIMO communications - a key to gigabit wireless," *Proc. IEEE*, vol. 92, no. 2, pp. 198–218, 2004.
- [34] H. Kazemi, Z. Mostaani, M. Uysal, and Z. Ghassemlooy, "Outage performance of MIMO free-space optical systems in gamma-gamma fading channels," in *18th European Conference on Network and Optical Communications (NOC), and 8th Conference on Optical Cabling and Infrastructure (OC&i)*, pp. 275–280.
- [35] Y. Liang, G. Xiqi, and M. S. Alouini, "Performance analysis of free-space optical communication systems with multiuser diversity over atmospheric turbulence channels," *IEEE Photon. J.*, vol. 6, no. 2, pp. 1–17, 2014.
- [36] A. Goldsmith, *Wireless Communications*. New York: Cambridge University Press, 2005.
- [37] H. Yang and M. Alouini, *Order Statistics in Wireless Communications: Diversity, Adaptation, and Scheduling in MIMO and OFDM Systems*. New York: Cambridge University Press, 2011.
- [38] A. S. Acampora and S. V. Krishnamurthy, "A broadband wireless access network based on mesh-connected free-space optical links," *IEEE Pers. Commun.*, vol. 6, no. 5, pp. 62–65, 1999.
- [39] N. D. Chatzidiamantis, D. S. Michalopoulos, E. E. Kriezis, G. K. Karagiannidis, and R. Schober, "Relay selection protocols for relay-assisted free-space optical systems," *IEEE J. Opt. Commun. Netw.*, vol. 5, no. 1, pp. 92–103, 2013.

- [40] J. Akella, M. Yuksel, and S. Kalyanaraman, "Error analysis of multi-hop free-space optical communication," in *IEEE International Conference on Communications (ICC)*, vol. 3, pp. 1777–1781 Vol. 3.
- [41] T. A. Tsiftsis, H. G. Sandalidis, G. K. Karagiannidis, and N. C. Sagias, "Multihop free-space optical communications over strong turbulence channels," in *International Conference on Communications (ICC)*, vol. 6, pp. 2755–2759.
- [42] M. Karimi and M. Nasiri-Kenari, "Outage analysis of relay-assisted free-space optical communications," *IET Commun.*, vol. 4, no. 12, pp. 1423–1432, 2010.
- [43] C. Abou-Rjeily, "Performance analysis of selective relaying in cooperative free-space optical systems," *J. Lightw. Technol.*, vol. 31, no. 18, pp. 2965–2973, 2013.
- [44] M. R. Bhatnagar, "Average BER analysis of relay selection based decode-and-forward cooperative communication over gamma-gamma fading FSO links," in *IEEE International Conference on Communications (ICC)*, pp. 3142–3147.
- [45] C. K. Datsikas, K. P. Peppas, N. C. Sagias, and G. S. Tombras, "Serial free-space optical relaying communications over gamma-gamma atmospheric turbulence channels," *IEEE J. Opt. Commun. Netw.*, vol. 2, no. 8, pp. 576–586, 2010.
- [46] M. Karimi and M. Nasiri-kenari, "Free space optical communications via optical amplify-and-forward relaying," *J. Lightw. Technol.*, vol. 29, no. 2, pp. 242–248, 2011.
- [47] E. Bayaki, D. S. Michalopoulos, and R. Schober, "EDFA-based all-optical relaying in free-space optical systems," *IEEE Trans. Commun.*, vol. 60, no. 12, pp. 3797–3807, 2012.
- [48] S. Kazemlou, S. Hranilovic, and S. Kumar, "All-optical multihop free-space optical communication systems," *J. Lightw. Technol.*, vol. 29, no. 18, pp. 2663–2669, 2011.
- [49] M. A. Kashani, M. M. Rad, M. Safari, and M. Uysal, "All-optical amplify-and-forward relaying system for atmospheric channels," *IEEE Commun. Lett.*, vol. 16, no. 10, pp. 1684–1687, 2012.
- [50] N. A. Olsson, "Lightwave systems with optical amplifiers," *J. Lightw. Technol.*, vol. 7, no. 7, pp. 1071–1082, 1989.
- [51] M. Razavi and J. H. Shapiro, "Wireless optical communications via diversity reception and optical preamplification," *IEEE Trans. Wireless Commun.*, vol. 4, no. 3, pp. 975–983, 2005.
- [52] R. Y. Mesleh, H. Haas, S. Sinanovic, A. Chang Wook, and Y. Sangboh, "Spatial modulation," *IEEE Trans. Veh. Technol.*, vol. 57, no. 4, pp. 2228–2241, 2008.

- [53] M. Di Renzo and H. Haas, "Bit error probability of SM-MIMO over generalized fading channels," *IEEE Trans. Veh. Technol.*, vol. 61, no. 3, pp. 1124–1144, 2012.
- [54] J. Jeganathan, A. Ghrayeb, and L. Szczecinski, "Spatial modulation: optimal detection and performance analysis," *IEEE Commun. Lett.*, vol. 12, no. 8, pp. 545–547, 2008.
- [55] M. Di Renzo, H. Haas, and P. M. Grant, "Spatial modulation for multiple-antenna wireless systems: a survey," *IEEE Commun. Mag.*, vol. 49, no. 12, pp. 182–191, 2011.
- [56] J. Jeganathan, A. Ghrayeb, L. Szczecinski, and A. Ceron, "Space shift keying modulation for MIMO channels," *IEEE Trans. Wireless Commun.*, vol. 8, no. 7, pp. 3692–3703, 2009.
- [57] W. O. Popoola, E. Poves, and H. Haas, "Spatial pulse position modulation for optical communications," *J. Lightw. Technol.*, vol. 30, no. 18, pp. 2948–2954, 2012.
- [58] T. Fath, H. Haas, M. Di Renzo, and R. Mesleh, "Spatial modulation applied to optical wireless communications in indoor LOS environments," in *IEEE Global Telecommunications Conference (GLOBECOM)*, pp. 1–5.
- [59] T. Ozbilgin and M. Koca, "Optical spatial pulse position amplitude modulation over atmospheric turbulence channels," in *International Conference on Communications (ICC)*, pp. 3412–3417.
- [60] M. Di Renzo and H. Haas, "Performance analysis of spatial modulation," in *5th International ICST Conference on Communications and Networking in China (CHINACOM)*, pp. 1–7.
- [61] M. Koca and H. Sari, "Generalized spatial modulation over correlated fading channels: Performance analysis and optimization," in *International Conference on Telecommunications (ICT)*, pp. 1–5.
- [62] R. Mesleh, H. Elgala, and H. Haas, "Optical spatial modulation," *IEEE/OSA J. Opt. Commun. Netw.*, vol. 3, no. 3, pp. 234–244, 2011.
- [63] R. Mesleh, S. Ikki, and M. Alwakeel, "Performance analysis of space shift keying with amplify and forward relaying," *IEEE Commun. Lett.*, vol. 15, no. 12, pp. 1350–1352, 2011.
- [64] R. Mesleh and S. S. Ikki, "Performance analysis of spatial modulation with multiple decode and forward relays," *IEEE Wireless Commun. Lett.*, vol. 2, no. 4, pp. 423–426, 2013.
- [65] I. Krikidis, J. S. Thompson, S. McLaughlin, and N. Goertz, "Max-min relay selection for legacy amplify-and-forward systems with interference," *IEEE Trans. Wireless Commun.*, vol. 8, no. 6, pp. 3016–3027, 2009.

- [66] S. Alexander, *Optical Communication Receiver Design*. Washington, USA: SPIE Press, 1997.
- [67] T. H. Carbonneau and D. R. Wisely, “Opportunities and challenges for optical wireless: the competitive advantage of free space telecommunications links in today’s crowded marketplace,” in *Wireless Technologies and Systems: Millimeter-Wave and Optical*, vol. 3232, pp. 119–128.
- [68] P. F. Szajowski, G. Nykolak, J. J. Auburn, H. M. Presby, and G. E. Tourgee, “High power optical amplifier enable 1550 nm terrestrial free-space optical data-link operating @ 10 gb/s,” in *IEEE Military Communications Conference (MILCOM)*, vol. 1, pp. 687–689 vol.1.
- [69] J. Peřina, “Superposition of coherent and incoherent fields,” *J. Phys. Lett. A*, vol. 24, no. 6, pp. 333–334, 1967.
- [70] M. O. Hasna and M. S. Alouini, “End-to-end performance of transmission systems with relays over rayleigh-fading channels,” *IEEE Trans. Wireless Commun.*, vol. 2, no. 6, pp. 1126–1131, 2003.
- [71] J. Proakis, *Digital Communications*. McGraw-Hill, 1995.
- [72] J. W. Craig, “A new, simple and exact result for calculating the probability of error for two-dimensional signal constellations,” in *Military Communications Conference (MILCOM)*, pp. 571–575 vol.2.
- [73] N. B. Mehta, W. Jingxian, A. F. Molisch, and Z. Jin, “Approximating a sum of random variables with a lognormal,” *IEEE Trans. Wireless Commun.*, vol. 6, no. 7, pp. 2690–2699, 2007.
- [74] M. Abramowitz and I. Stegun, *Handbook of Mathematical Functions: With Formulas, Graphs, and Mathematical Tables*. USA: U.S. Department of Commerce, National Bureau of Standards, 1972.

VITA

Zohreh Mostaani received her B.Sc. degree in electrical and computer engineering from University of Tehran, Tehran, Iran, in 2011. She is currently a M.Sc. student at Electrical and Electronic engineering department of Özyeğin University, Istanbul, Turkey and a member of Communication Theory and Technology (CT&T) research group under supervision of Professor Murat Uysal. Her research is in the area of MIMO, diversity techniques, spatial modulation, relay-assisted communication and all-optical relaying in Free Space Optical Communication.